International Journal of Nanomedicine

Dovepress
open access to scientific and medical research

Open Access Full Text Article

ORIGINAL RESEARCH

Nanoporous solid-state membranes modified with multi-wall carbon nanotubes with anti-biofouling property

This article was published in the following Dove Medical Press journal:
International Journal of Nanomedicine

Ameneh Alizadeh[1]
Amir Razmjou[1,2]
Mehrorang Ghaedi[3]
Ramin Jannesar[4,5]

[1]Department of Biotechnology, Faculty of Advanced Sciences and Technologies, University of Isfahan, Isfahan 8174673441, Iran; [2]UNESCO Centre for Membrane Science and Technology, School of Chemical Science and Engineering, University of New South Wales, Sydney 2052, NSW, Australia; [3]Department of Chemistry, Yasouj University, Yasouj 75918-74831, Iran; [4]Department of Pathology, Yasuj University of Medical Sciences, Yasuj 7591741417, Iran; [5]Department of Biotechnology and Microbial Nanotechnology, Dena Pathobiology Laboratory, Yasuj 7591774414, Iran

Purpose: Nanoporous membranes have been employing more than before in applications such as biomedical due to nanometer hexagonal pores array. Biofouling is one of the important problems in these applications that used nanoporous membranes and are in close contact with microorganisms. Surface modification of the membrane is one way to prevent biofilm formation; therefore, the membrane made in this work is modified with carbon nanotubes.

Methods: In this work, nanoporous solid-state membrane (NSSM) was made by a two-step anodization method, and then modified with carbon nanotubes (NSSM-multi-wall carbon nanotubes [MWCNT]) by a simple chemical reaction. Techniques such as atomic force microscopy (AFM), energy dispersive X-ray (EDAX), field emission scanning electron microscopy (FESEM), Fourier-transform infrared spectroscopy (FTIR), contact angle (CA), surface free energy (SFE), protein adsorption, flow cytometry, and MTT assay were used for membrane characterization.

Results: The BSA protein adsorption capacity reduced from 992.54 to 97.24 ($\mu g\ mL^{-1}\ cm^{-2}$) after modification. The findings of flow cytometry and MTT assay confirmed that the number of dead bacteria was higher on the NSSM-MWCNT surface than that of control. Adsorption models of Freundlich and Langmuir and kinetics models were studied to understand the governing mechanism by which bacteria migrate to the membrane surface.

Conclusion: The cell viability of absorbed bacteria on the NSSM-MWCNT was disrupted in direct physical contact with carbon nanotubes. Then, the dead bacteria were desorbed from the surface of the hydrophilic membrane. The results of this research showed that NSSM-MWCNT containing carbon nanotubes have significant antimicrobial and self-cleaning property that can be used in many biomedical devices without facing the eminent problem of biofouling.

Keywords: anodizing, alumina anodic membrane, antibacterial, anti-biofilm

Introduction

Membranes are used in biomedical, biological, chemical, and industrial applications. Self-ordered monodisperse nanoporous solid-state membranes (NSSM) with a hexagonal structure have been used more frequently than before in medical applications.[1] These membranes with unique designs, nanometer pores, uniformity, high porosity, proper thickness, and high aspect ratio are used in many biomedical processes.[2,3] Alumina membranes with uniform pore size have been utilized for a large variety of biological uses for instance, DNA filtering and detection,[4,5] cell culture,[6] biosensor,[7] and microfluidic chips. NSSM-based microfluidic chip systems allow the detection of a large variety of bacteria simultaneously.[8] Recently, NSSM have been integrated with ordinary biosensors for lab-on-a-chip applications.[9] For biological and medical applications of such membranes, biocompatibility, and physical and chemical stability

Correspondence: Amir Razmjou
Department of Biotechnology, Faculty of Advanced Sciences and Technologies, University of Isfahan, Hezar Jarib Street, Isfahan 8174673441, Iran
Tel +98 31 3793 4401
Email razmjou@ast.ui.ac.ir

Mehrorang Ghaedi
Department of Chemistry, Yasouj University, Pasdaran Street, Yasouj 75918-74831, Iran
Tel +98 91 7122 4331
Email m_ghaedi@mail.yu.ac.ir

submit your manuscript | www.dovepress.com
Dovepress
http://dx.doi.org/10.2147/IJN.S189728

are considered critical properties. Membrane biofouling (biofilm) is a serious problem in biomedical applications, since microorganisms including protein compounds and bacteria are nonspecifically adsorbed into the surface and can multiply, even if most of them have been removed. Biofouling can create a major problem in biomedical applications such as increasing infections caused by medical devices and decreasing antimicrobial effectiveness.[10] One way to reduce and prevent biofilm formation is surface modification of the sample which can prevent the growth of microorganisms.[11] Researchers have used various biocompatible materials to improve the surface of NSSM such as polymers and proteins.[6,12–15] The surface modification method preserves the nanoporous structure of NSSM and improves chemical, physical, and biological properties. However, none of them have shown satisfying anti-biofouling efficacy.

Carbon-based materials with various physical and chemical properties have exhibited great potential for many biomedical applications.[16] The addition of a small amount of carbon nanotube into mixed matrix membranes lead to the formation of nanocomposites with improved mechanical, physical, and antimicrobial properties.[17–19] Also, many researchers have proven that carbon has antimicrobial properties which eliminate bacterial and viral infections.[20–22] Carbon nanotube membranes can remove almost all types of contaminations of water, food, and dairy including bacteria, viruses, microbes, fungi, organic compounds, and heavy metals.[23,24]

However, using carbon nanotubes for surface modification of solid-state membranes for industrial and biomedical applications has not been fully explored yet. Here, we designed our surface treatment strategy based on the fact that the nano-scale edges of the multi-walled carbon nanotube (MWCNT) can enter the outer surface of microorganisms which results in superoxide anion damage.[25] In this project, NSSM were made by a two-step anodization method and then modified with hydrophilic carbon nanotubes. Different analytical techniques were used to characterize unmodified and modified membranes. It is well proven that *Staphylococcus aureus* and *Escherichia coli* can form biofilm on the sample surface.[10] The impact of membrane modification on the reduction of biofilm was investigated with the immersion of membranes into the suspension of the two bacteria, and then it was analyzed by scanning electron microscopy (SEM). Multi-walled carbon nanotubes with antimicrobial properties can penetrate the outer membrane of bacteria, destroying cell viability. Dead bacteria were removed from the surface with the increment of water layers and repulsive forces. Therefore NSSM-MWCNT surface does not form biofilm.[26]

Materials and methods

Materials

All of the solutions were prepared in double-distilled water. Oxalic acid, phosphoric acid (85%), perchloric acid (70%), hydrochloric acid (37%), nitric acid (63%), sulfuric acid, hydrogen peroxide (30%), ethanol (95.5%), methanol (95%), acetone, chromic oxide, sodium hydroxyl, copper chloride (II), brilliant blue G, glycerol, and dimethyl sulfoxide were provided by EMD Millipore (Billerica, MA, USA). Crystal violet and aluminum foil (99.99%) were bought respectively from Cib Biotech Co (Tehran, Iran) and Kingcheng (Shanghai, China). NaH_2PO_4, Na_2HPO_4, BSA, and MTT reagents were provided by Sigma-Aldrich Co. (St Louis, MO, USA). MWCNT (outer diameter: 8–15 nm) was bought from CheapTubes.com (Cambridgeport, VT, USA). Two strains of bacteria containing *E. coli* ATCC: 25922 and *S. aureus* ATCC: 25923 as biofilm former were provided by Pasteur Institute of Iran (Tehran, Iran).

Preparation of membranes

Al foil (99.99%) was cut into small pieces of 1×1 cm and annealed by a tubular furnace (HYSC model, automatically) at 600°C for 5 hours. Then, the aluminum discs were degraded by sonication in acetone/water for 3 minutes. The cleaned aluminum discs were electropolished in a mixture of $HClO_4$ and C_2H_5OH at a ratio of 1:4 (vol) at 20 V (MEGATEK, 0–250 V, 0–30 mA) for 3 minutes. Afterward, the first-step anodization was done using aqueous solutions of $H_2C_2O_4$ (0.3 M) and H_3PO_4 (0.2 M) at 100 V, 24°C for 1 hour. The first anodic layer was removed by H_3PO_4 (6%) and H_2CrO_4 (1.8%) at 65°C for 1 hour in a water bath (HYSC model, automatically). The next step of anodization was performed using the electrolyte and voltage conditions of the first step for 5 hours. The remaining aluminum was etched with an H_2O-HCl–$CuCl_2$ mixed solution. In the next step, the barrier layer was dissolved by using H_3PO_4 5%. For the hydroxylation of NSSM, the membranes were immersed in H_2O_2 solution (30%), then they were placed in an ultrasonic bath at 70°C for 1 hour and cleaned by deionized H_2O. Afterward, the membranes were desiccated in an oven for 3 hours at 100°C. At this step, the membrane was hydroxylated. For surface modification of NSSM with carboxylated MWCNT, 1 mg carboxylated MWCNT was thoroughly dispersed in 20 mL deionized water under sonication for 1 hour. Then, drops of MWCNT dispersion were poured on the hydroxylated membrane surface and dried at room temperature (Figure S1 shows schematically, the membrane preparation and modification procedure).

Membranes' characterization

To determine functional groups of the membranes, Fourier-transform infrared spectroscopy (FTIR) (FTIR-8300 spectrophotometer, Shimadzu Co. Tokyo, Japan) analysis was done with a KBr disk. The samples were fixed on the holder, and the transmittance spectrum from 400–4,000 cm^{-1} was scanned. The morphology of membranes was characterized by FESEM (Stereo Scan S360 Cambridge instrument, Cambridge, England), FESEM (ZEISS SIGMA VP, Berlin, Germany), and FESEM (TESCAN MIRA3, Prague, Czechoslovakia). The existence of MWCNT in the membrane was analyzed by energy dispersive X-ray (EDAX) point and mapping (Hitachi S3400, Hitachi Ltd., Tokyo, Japan). The roughness was determined by AFM (Dualscop C-26 DME, Berlin, Germany). The samples were scanned by tapping mode at 500×500 nm. The effect of treatment on the samples' wettability was checked out by water contact angle (CA) (θ°) measurements system model OCA 15 plus. The surface of the samples was characterized using sessile drop methods. Ten microliters of water were poured on the chosen area of samples, and the average CA of six different positions was reported for each sample. The surface free energy (SFE) of the specimen was acquired by the Van-Oss approach. The images at 5-minute intervals were obtained, and the average of six measurements for each sample was reported. H_2O_2, $C_3H_8O_3$, and CH_3NO with specified parameters (Table S1) were used to compute the SFE of the samples.[27,28] An in-house dead-end device was utilized to evaluate the water flux. The pure H_2O fluxes were obtained as J (mL/cm^2 min). To measure BSA rejection, the solution of BSA with a specific initial concentration was passed through the embedded membranes in the dead-end device, then the concentration of permeate solution was determined. The BSA concentration was obtained by UV-visible spectrophotometry. The rejection ratio (R) was estimated as indicated in the following formula:[29]

$$R\ (\%) = \left[\left(1 - \frac{C_p}{C_f}\right)\right] \times 100 \qquad (1)$$

In the equation $C_{p,f}$ are protein concentrations; index of p stands for permeate while f stands for feed solutions.

Protein adhesion test

The impact of membrane treatment with MWCNT on the proteins' adsorption of the samples was examined by Bradford assay. Modified and unmodified membranes (4 mm in diameter) were maintained in a 1 mg/mL BSA solution (pH of 7.4) for 4 hours. Then the absorbance was acquired at 555 nm using UV-visible spectrophotometry (V-570 Jasco Co., Hachioji, Tokyo, Japan) after removing the specimens. The quantity of the adsorbed BSA on the samples was evaluated according to Razmjou et al.[30,31]

Bacterial attachment test (biofilm assay)

E. coli and *S. aureus* were selected to investigate the formation of biofilm. *E. coli* has become a prominent model organism for biofilm research. *E. coli* strains have become notorious pathogens causing a broad spectrum of diseases and pose a significant risk to human health worldwide. Also, the capacity of *S. aureus* to form biofilm is an important virulence factor in the development of device-related infections.[32–34] The bacterial strains were cultured overnight in a Muller Hinton broth medium (MHBM) at 37°C at 150 rpm. The overnight bacterial suspensions were diluted with fresh and sterilized MHBM to adjust the half-McFarland standards by measuring the absorbance at 625 nm.[35] The specimens were sterilized with ethanol 75% and were dried near the flame. Then, unmodified and modified membranes were immersed inside the test tubes comprising a suspension of bacteria and were incubated for 10 days. After 10 days, 2 mL of methanol (99% v/v) was added to each sample. Two milliliters of crystal violet (0.3%) was added to samples to stain bacteria. After 5 minutes' incubation at 25°C, samples were rinsed many times with deionized H_2O and finally, the samples were analyzed by SEM.

Flow cytometry

Flow cytometry was applied to study the impact of the modification on the integrity of the cell membrane. Cell particles and cell adhesion were analyzed via flow cytometry method. The bacterial suspension of *E. coli* and *S. aureus* (1.5×10^8 CFU/mL) were made according to the previous step. The specimens were sterilized; then they were incubated in a plate including bacterial suspensions, at 37°C overnight. Then, the samples and fresh MHBM were sonicated for 30 seconds to create a optimum bacterial concentration. To identify dead and alive cells; 5 µL of propidium iodide (1 mg/mL) was added to a combination of the sample (50 µL) and the deionized water (5 mL). After 10 minutes' incubation in the dark, the levels of bacterial adhesion were investigated with flow cytometry technique (BD Biosciences, San Jose, CA, USA), and were interpreted by Flowjo software. The test was calibrated with live and dead cells of the bacteria to provide information about the location and aggregation of the dead, live, and injured cells.[36,37]

MTT assay

MTT assay is a colorimetric technique to evaluate cell viability. Microbial suspensions were prepared with the concentrations of 10^5, 10^6, 10^7, and 10^8 CFU/mL. The membrane samples were placed in the dead-end cell and bacterial suspension was passed through sterilized membranes using a pump at 0.05 mL per minute. Then, 10 µL of the microbial suspension which was passed through the membrane was poured in the 96-well plate, 5 µL of the MTT reagent was added and it was incubated at 37°C for 1 hour. After the formation of purple sediment of formazan, dimethyl sulfoxide was added to cell's culture media and incubated for 1 hour. Finally, the absorption at 570 nm was determined by a plate reader (Synergy HTX, BioTE, OTT, Canada).

The effect of absorption process on the reduction of biofilm

Initially, the MHBM was used and autoclaved at 121°C for 15 minutes. The same amount of 4–5 colonies from the 24-hour *E. coli* fresh microbial culture was placed in a tube containing 5 mL MHBM to obtain a microbial suspension, then they were cultured in MHBM at 37°C for 24 hours. The bacterial suspensions were diluted with fresh and sterilized MHBM to adjust the half-McFarland standard by considering the absorbance at 625 nm. The membranes were placed in the dead-end device. Then, the prepared bacterial suspension was passed through the membranes by a syringe pump SP1000 (Fanavaran Nano-Meghyas Co., Tehran, Iran). The permeation was cultured in Muller Hinton agar medium for 24 hours at 37°C (Figure S2). The kinetic models at the different contact times and at the concentration of 1.5×10^8 CFU/mL of *E. coli* were investigated. The isotherm studies were examined at various initial concentrations of *E. coli* and equilibrium time. Then the Freundlich ($Logq_e$ vs $Logc_e$) and Langmuir (c_e/q_e vs c_e) isothermal models were used. The retained amounts of *E. coli* in the suspension were measured with the plate count method (Figure S3). In the method, 90 µL of MHBM was poured into the first row of the dilution plate. Then, 10 µL of bacterial suspension which was passed through the membranes was added to the first well of the dilution plate (dilution of 1:10). Then, 10 µL of the first well was poured into the second well, and it was continued to the fifth well (dilutions of 1:100, 1:1,000, 1:10,000, 1:100,000). Diluted samples were cultured onto Muller Hinton agar to assess the number of colonies by a colony counter (TAT-Ko, Teifazmateb,Tehran). To count the number of bacteria on the plate, the following formula was used:[38]

$$N \times b = m \quad (2)$$

In the equation N is a count of colonies, b is a reciprocal dilution of sample and m is the number of bacteria/mL. The amount of *E. coli* absorbed by membranes, q_e (CFU/g), was obtained as follows:

$$q_e = (C_0 - C_e) \times L/G \quad (3)$$

In the formula C_0 and C_e are the initial and residual concentration of bacteria (CFU/mL), G is the mass of membrane, and L is the suspension volume. The impact of temperature in adsorption of *E. coli* was investigated by using initial *E. coli* concentrations of 1.5×10^8 CFU/mL for 5, 10, 15, 20 and 30°C, The thermodynamic parameters for the adsorption of *E. coli* by NSSM-MWCNT such as enthalpy (ΔH), the Gibbs free energy (ΔG), and entropy (ΔS) changes were determined to evaluate the thermodynamic feasibility and spontaneous nature of the process by using the following equations:

$$\mathrm{LnKc} = \frac{\Delta S}{R} - \frac{H}{RT} \quad (4)$$

$$G = H - TS \quad (5)$$

where ΔS is entropy change (kJ/mol.k), ΔH is enthalpy changes (kJ/mol), R is the universal gas constant (8.314 J/mol Kol), Kc is the thermodynamic equilibrium constant, and T is the absolute temperature (K).[39,40]

Results and discussion

Membrane characterization

The prepared NSSM is clear and can be studied in the infrared region.[41] The FTIR of NSSM (Figure 1a), showing

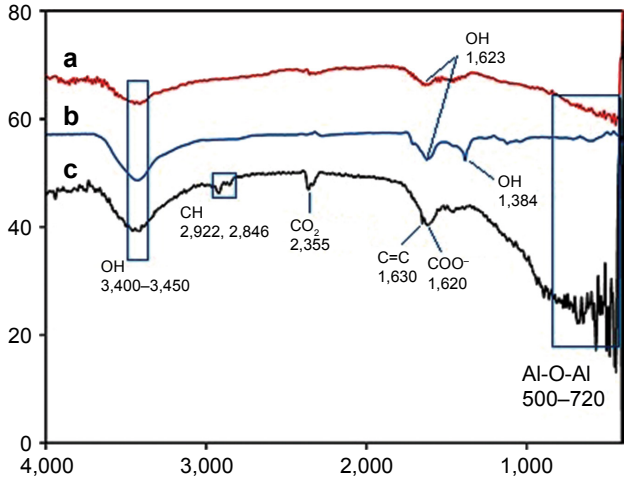

Figure 1 FTIR spectrum of membranes: **a:** NSSM, **b:** NSSM-OH, **c:** NSSM-MWCNT.
Abbreviations: FTIR, Fourier-transform infrared spectroscopy; MWCNT, multi-walled carbon nanotube; NSSM, nanoporous solid-state membrane.

adsorption peaks around 1,623 and 3,450 cm^{-1}, is indicative of the H_2O molecule. The first peak is attributed to the bending vibration of the H_2O and the second is the stretching vibration of the O-H bond that comes from coordinated water on the NSSM surface.[42] The characteristic peaks at 514 cm^{-1} and 720 cm^{-1} are due to the stretching vibrations of Al-O-Al in Al_2O_3.[43] The FTIR of the NSSM-OH (Figure 1b) showing adsorption peaks around 1,384, 3,450, and 1,623 cm^{-1} corresponds to the vibrations of the hydroxyl group.[44] The hydroxyl group on the NSSM surface is expected to increase after the H_2O_2 pretreatment process. The FTIR spectra of the NSSM-MWCNT (Figure 1c) membranes exhibited peaks on 2,846 and 2,922 cm^{-1} of C-H stretch mode, 1,630 cm^{-1} of C=C, 1,620 cm^{-1} of COO^- and 2,355 cm^{-1} of CO_2.[45,46] Comparatively, the spectra of NSSM and NSSM-H_2O_2 membranes did not show the C-H vibration stretch mode. The NSSM-MWCNT membranes showed carboxylate vibration, which indicates the proton dissociation of carboxylic acid to form carboxylates. The carboxylate groups of carbon nanotubes are attached to NSSM surface through hydrogen bonding with hydroxyl ions from the alumina.[47,48] Figure 2A and B present the EDX data and the image of NSSM. The presence of the characteristics of X-ray peaks O (K=0.50 keV) and Al (K=1.50 keV) provides insight into the elemental combination of the nanoporous AL_2O_3 membrane and its high purity. Also, the EDX results (Figure 2C) display the existence of

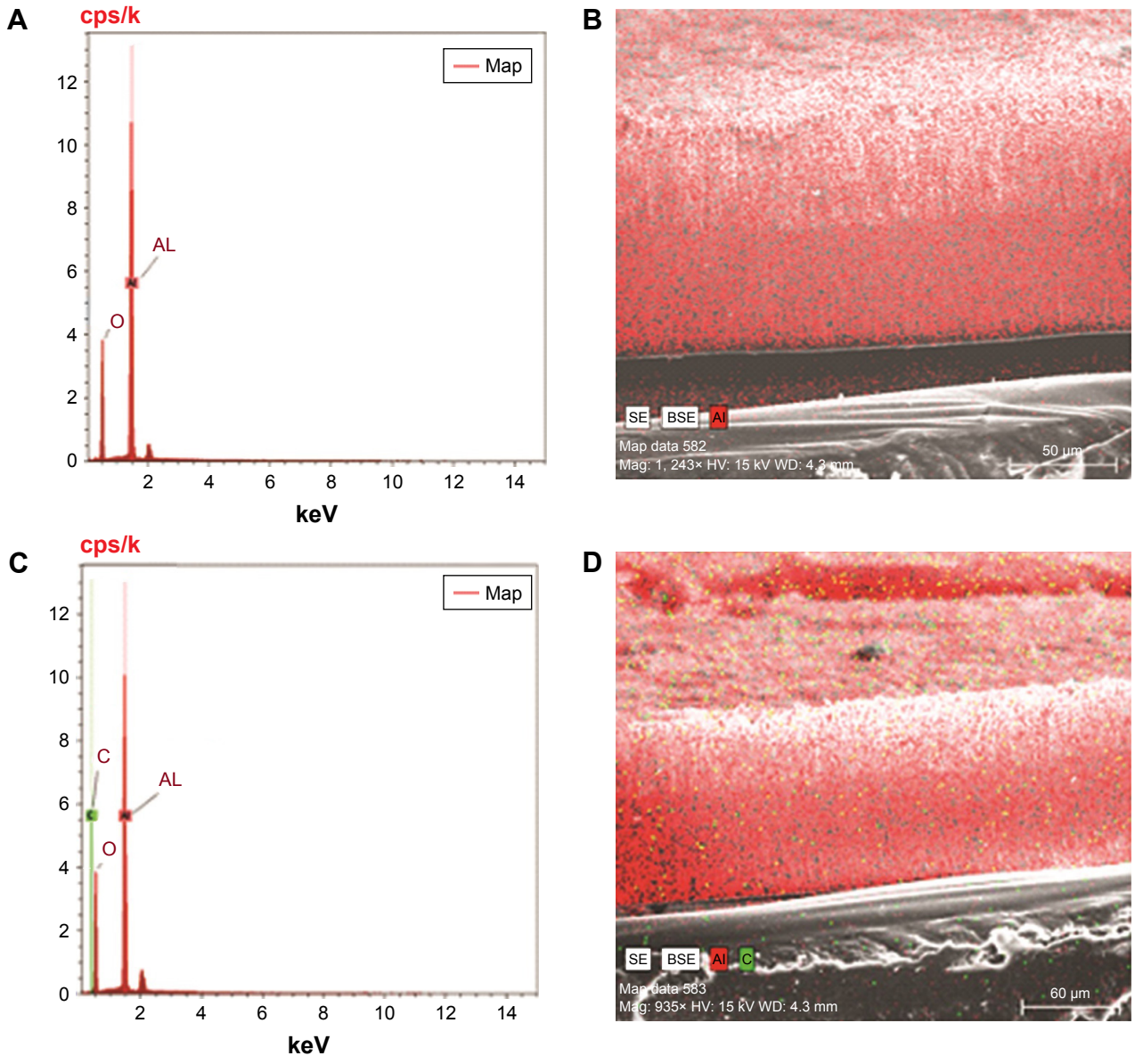

Figure 2 EDAX point data and EDAX image of membrane (**A**, **B**) NSSM, (**C**, **D**) NSSM-MWCNT which were anodized in aqueous solutions of acid, 100 V and 25°C.
Abbreviations: EDAX, energy dispersive X-ray; MWCNT, multi-walled carbon nanotube; NSSM, nanoporous solid-state membrane.

C (0.27 keV), O (0.50 keV) and Al (1.50 keV). The EDX image (Figure 2D) confirms the existence of carbon nanotubes on the surface and inside pores, but it shows that MWCNTs appear near the surface rather than inside the pores. This was expected because of appearance of more OH on the surface. Figure 3A shows a surface image of the membrane with highly ordered nano-scale pores (200–300 nm) with hexagonal arrangement. The SEM studies showed that the pores were homogenously distributed over the membranes. Cross-section SEM image (Figure 3B) shows that the structure of NSSM included vertically cellular and cylindrical pores. Also, it was revealed that the nano-channels were parallel. Figure 3C exhibits that the carbon nanotube, through the carboxyl groups at its end, reacts with hydroxyl groups of the membrane, and forms hydrogen bonding. To confirm the existence of carbon inside the nanopores, an NSSM-MWCNT membrane was broken in half, and its cross-section was analyzed by SEM (Figure 3D). Different areas, close to the surface, and far from the surface were analyzed and it was confirmed that the surface and inside of the membrane were covered with carbon nanotubes. The roughness of the surface has an important effect on the anti-fouling property as the microorganisms want to block the valley of samples.[42–44] Figure 4A and B show the image of two-dimensional and three-dimensional AFM of ordered NSSM with hexagonal cells with central circular nanopores. In AFM technique, no conductivity is required.[45] Figure 4C and D show the AFM two-dimensional and three-dimensional images of NSSM-MWCNT. The AFM analysis on the area with 500×500 nm size displayed that the roughness (Ra) of the sample was increased from 11.2 nm for NSSM, which was reported earlier,[42] to 52.0 nm for NSSM-MWCNT. AFM measurement confirmed the results of SEM and determined the average amount of roughness. Figure 4E and F show the AFM three-dimensional images of NSSM and NSSM-MWCNT on the regions of 100×100 nm. The mean nanoroughness (Ra) of the membrane increased for NSSM-MWCNT from 9.0–65 nm. According to the Wenzel model, with increasing roughness, the hydrophilic nature of a surface can shift toward superhydrophilicity.[46] Water layers increase with the increasing hydrophilicity, and these layers wash bacteria damaged by MWCNT from the surface, thus avoiding the formation of biofilm.[47]

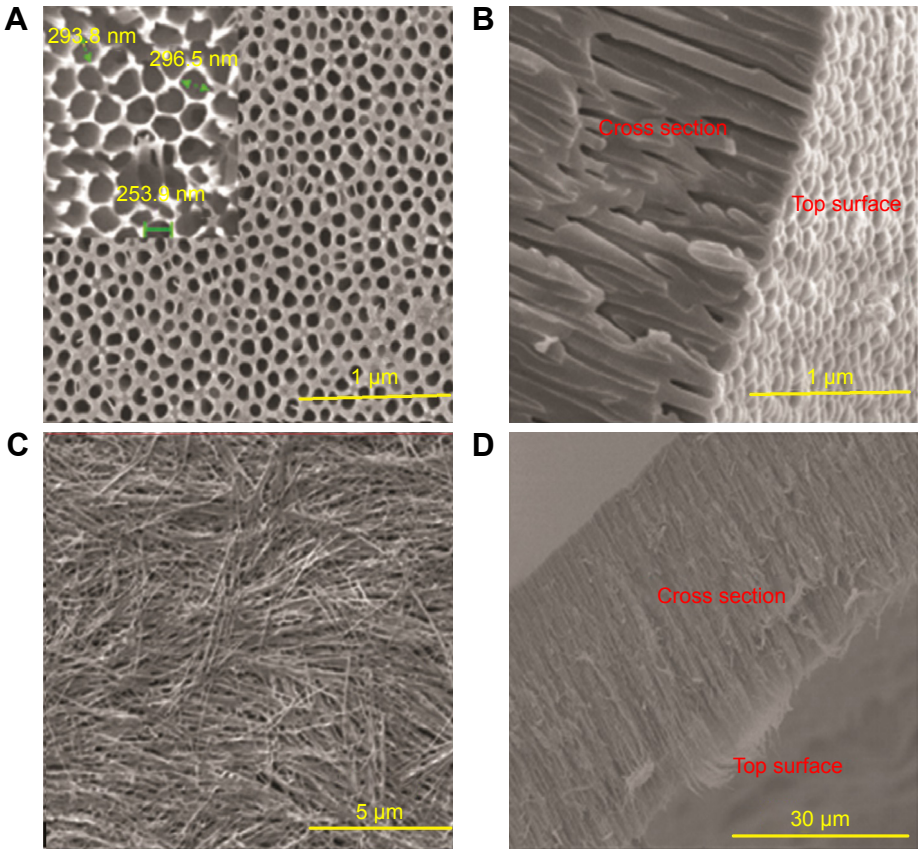

Figure 3 SEM image of surface and cross-section (**A**, **B**) of NSSM and (**C**, **D**) NSSM-MWCNT membranes which were anodized in aqueous solutions of acid, 100 V and 25°C.
Abbreviations: MWCNT, multi-walled carbon nanotube; NSSM, nanoporous solid-state membrane; SEM, scanning electron microscopy.

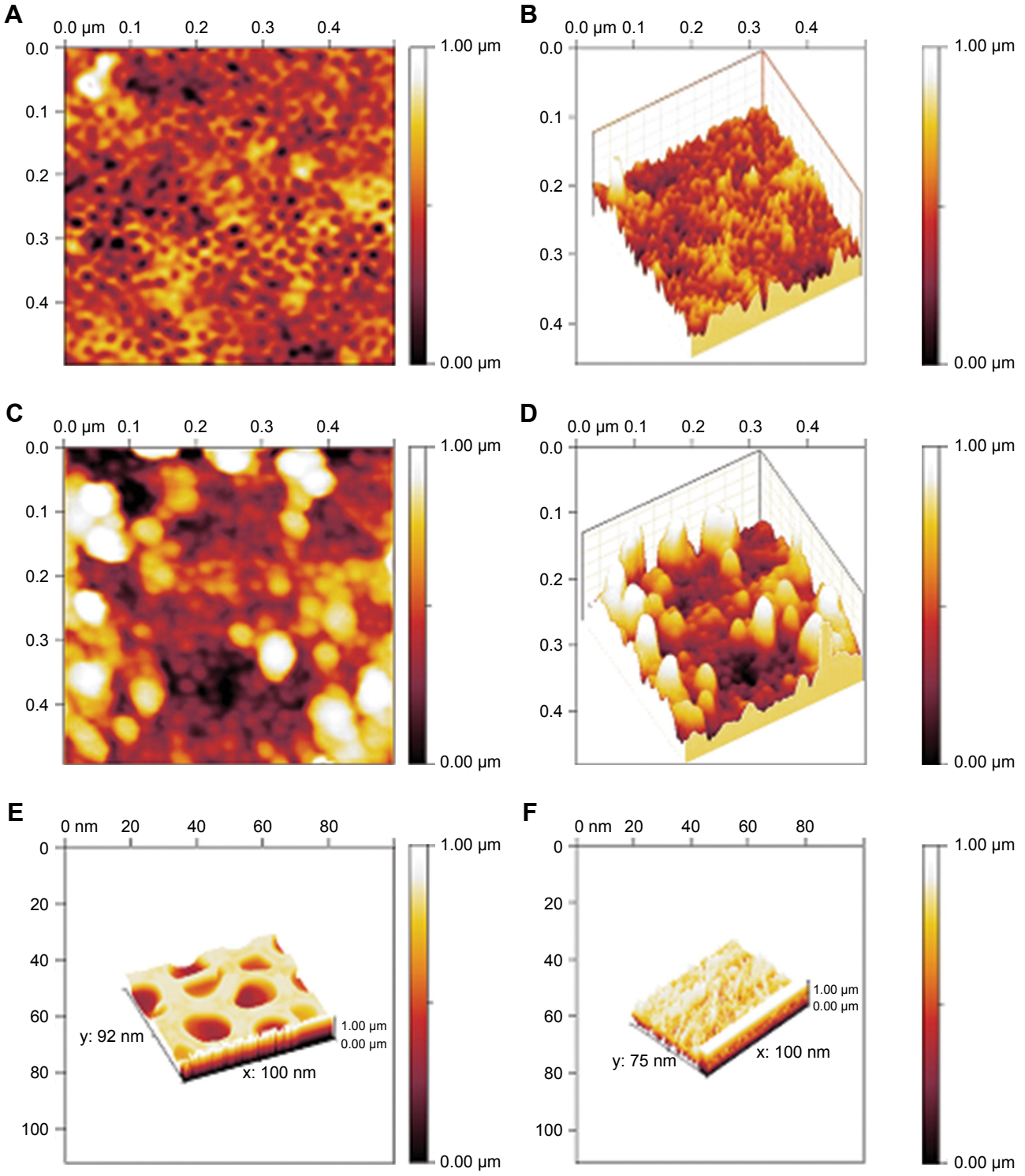

Figure 4 AFM: two-dimensional (**A** and **B**) three-dimensional images of NSSM, (**C**) two-dimensional and (**D**) three-dimensional images of NSSM-MWCNT (500×500 nm), (**E**) three-dimensional images of NSSM and (**F**) NSSM-MWCNT (100×100 nm).
Abbreviations: AFM, atomic force microscopy; MWCNT, multi-walled carbon nanotube; NSSM, nanoporous solid-state membrane.

CA and SFE

The two computations of CA and SFE are applied to study membrane surface wettability and anti-biofouling properties.[43] Hydrophilic membranes are preferred because of lower protein molecule absorption.[48] The wettability parameter that is reported by CA (θ) is determined by the interaction of adhesive and cohesive forces at interfaces of solid, liquid, and vapor phases. The relationship between

the spreading of the drop on the surface and the SFE is the opposite.[49] A water droplet follows the profile of the specimen, as shown by Wenzel.[46]

$$\mathrm{Cos}\theta_w = \mathrm{r}\,\mathrm{Cos}\theta_e \quad (6)$$

where $\theta_{w,e}$ are the obvious angles and on the plane area respectively. The r is the relation of the solid real area to geometric design.[45] In Equation 6, the increment of nanoroughness can alter a hydrophilic surface to a superhydrophilic one.[25] In this project, the modification of NSSM shifts the water CA from 30°–9°. MWCNT can create hydrophilic groups on the surface and increase nanoroughness, therefore it can improve the hydrophilicity of the modified sample. Our calculation showed that the modification increased the SFE from 181.76 for NSSM to 260.64 (mN/m) for MWCNT-NSSM, which could be related to higher density of hydroxyl groups on the NSSM-MWCNT surface (Figure 5). Membranes with less water contact angle and higher SFE have fewer interactions with the microorganism. Since hydrophilic surfaces have repulsive forces on the foulant absorption, they will have a better anti-biofouling performance.[48]

Membrane performance (water flux)

Water flux from 0.12 for NSSM increased to 0.53 mL/cm^2 min for NSSM-MWCNT. It is proven that the higher hydrophilicity, the greater pure water flux.[31] The high SFE and roughness of the sample could have simultaneously contributed to this finding. Also, the rejections of BSA for the modified and unmodified membranes were 99% and 89% respectively.

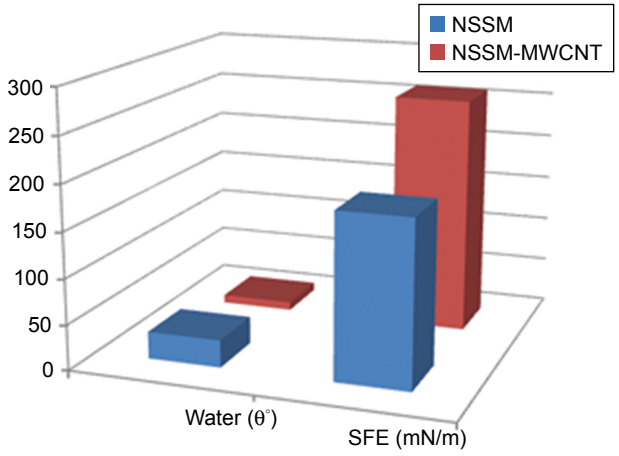

Figure 5 WCA and SFE of NSSM and NSSM-MWCNT membranes.
Abbreviations: MWCNT, multi-walled carbon nanotube; NSSM, nanoporous solid-state membrane; SFE, surface free energy; WCA, water contact angle.

Based on the results of various analyses including FTIR, EDAX, SEM, and AFM, the surface of NSSM-MWCNT is rougher, more porous, has higher specific surface area and functional groups as well as smaller pore size than NSSM, so NSSM-MWCNT must be able to absorb more bacteria. Due to the antibacterial properties of carbon nanotubes, we expected that the modified membrane with higher bacterial absorption capacity could damage the outer layers of cell membranes. Finally, the water layers on the modified membrane surface would eliminate the disrupted bacteria off the surface. For further investigation, we carried out more biological tests.

Protein adsorption resistance

In this work, investigating the impact of the modification on the sample's anti-fouling property was performed by BSA adsorption test. NSSM-MWCNT membrane showed lower protein adsorption compared to NSSM, which indicates a salient increase in the biofouling resistance. Protein adsorption for unmodified and modified membranes was 992.54 and 97.24 μg mL^{-1} cm^{-2}, respectively. This significant reduction in protein adsorption is due to the addition of hydrophilic MWCNT and increase in nanoroughness. Water barrier mechanism leads to lower protein adsorption for NSSM-MWCNT.[50–52] Lower protein adsorption can lead to biofilm reduction, which will be investigated in the next section.

Bacterial attachment (biofilm assay)

Two strains of bacteria containing *E. coli* and *S. aureus* were selected to investigate biofilm formation. Modification of alumina membrane by MWCNT reduced the biofilm. In Figure 6A (5.00 kx) and B (200.00 kx) of the surface, SEM images show that biofilm was formed on the unmodified membrane. Rod-shaped[53] and spherical-shaped (grape-like clusters)[54] bacteria on the NSSM are attributed to *E. coli* and *S. aureus* respectively. Intermediate wettability generates a situation for proteins to accumulate and nucleate inside the pores.[49] The dwell time of BSA (dimensions: 14×3.8×3.8 nm)[55] proteins entering the membrane pores is longer than their leaving time and thus the distance of protein-protein is reduced and provides an opportunity for other proteins to enter, which leads to the growth of protein adsorption on the samples.[56] In Figure 6C (30.00 kx) and D (50.00 kx), SEM images of the surface show that biofilm did not appear on the surface of the MWCNT-NSSM because MWCNT with inherent antimicrobial properties increased the roughness and hydrophilicity of the membrane. Therefore, modified membranes can be used in biomedical applications

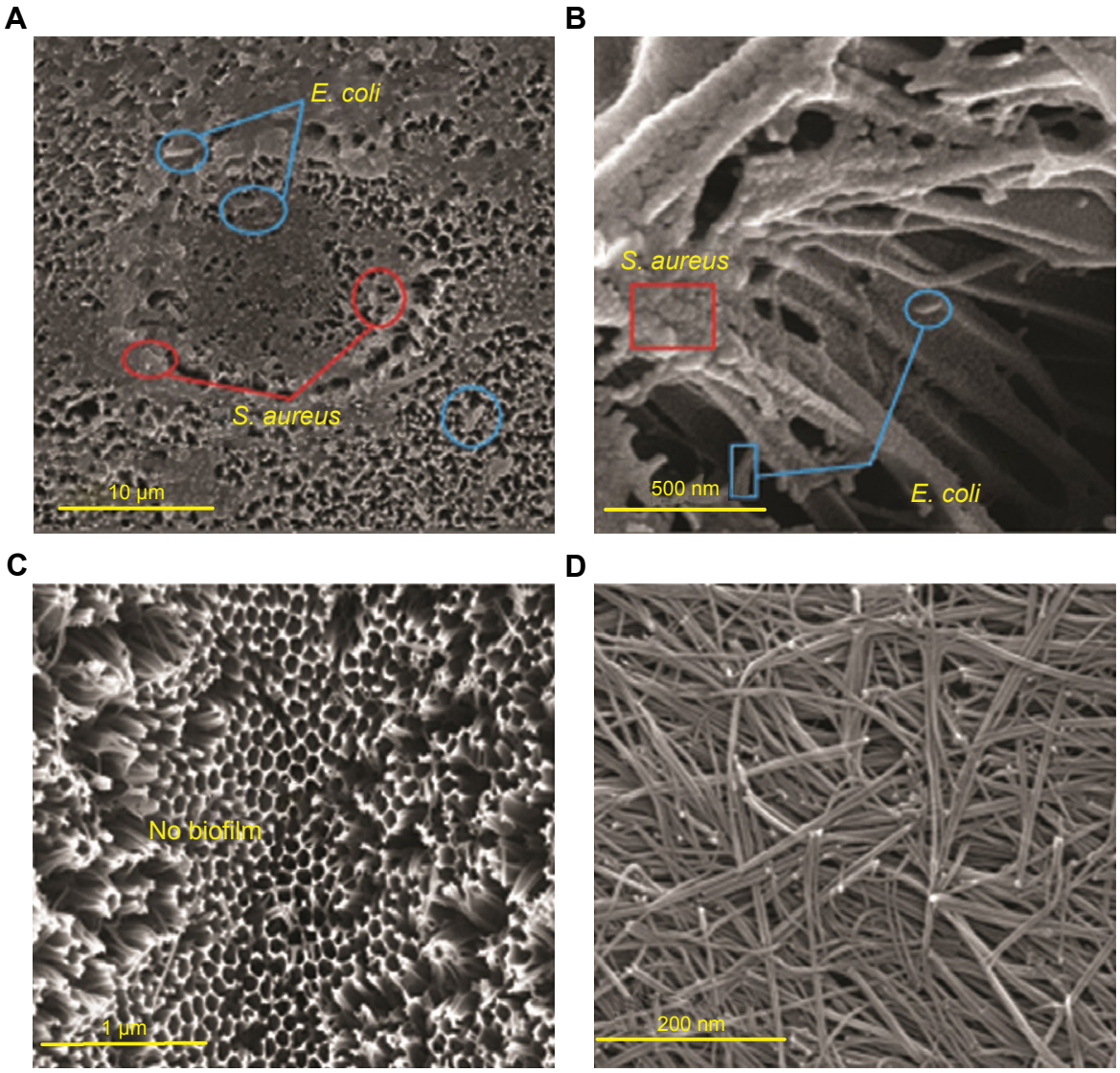

Figure 6 Surface SEM image of NSSM (**A**) 5.00 kx, (**B**) 200 kx, and NSSM-MWCNT (**C**) 30.00 kx and (**D**) 50.00 kx after biofilm assay.
Abbreviations: *E. coli*, *Escherichia coli*; MWCNT, multi-walled carbon nanotube; NSSM, nanoporous solid-state membrane; SEM, scanning electron microscopy; *S. aureus*, *Staphylococcus aureus*.

such as cell culture, or industrial applications such as reducing the microbial load of dairy products and wastewater treatment.[57–59] We performed MTT assay and flow cytometry tests to confirm the SEM results and also to evaluate the formation of biofilm on the surface of the membrane. Figure 7 indicates the finding of flow cytometry assay for (A) NSSM-*E. coli*, (B) NSSM-*S. aureus*, (C) NSSM-MWCNT-*E. coli*, and (D) NSSM-MWCNT-*S. aureus*. The results indicated that the maximum dead bacteria were dedicated to NSSM-MWCNT membrane. Remarkably, >98% of the bacteria were killed by NSSM-MWCNT membranes. The MTT reagent is a dye for the study of viability and cytotoxicity based on the oxidation-reduction reaction; this method is based on the activities of cytoplasmic enzymes of living bacteria. The findings of the MTT test are presented in Figure 8 for the NSSM and NSSM-MWCNT specimens. The percentage of bacteria viability for the control sample in each of the four concentrations is higher than 91% and for the modified membrane is less than 4%.

The nanoroughness and hydrophilicity enhancement can limit the reaction between the membrane and the microorganism which results in the reduction of adhesion trend. The bacteria are absorbed on the carbon nanotubes due to a cylindrical shape, high aspect ratio, and functional groups such as OH and COOH. Upon bacterial attachment, their cell membrane is damaged in direct contact with carbon

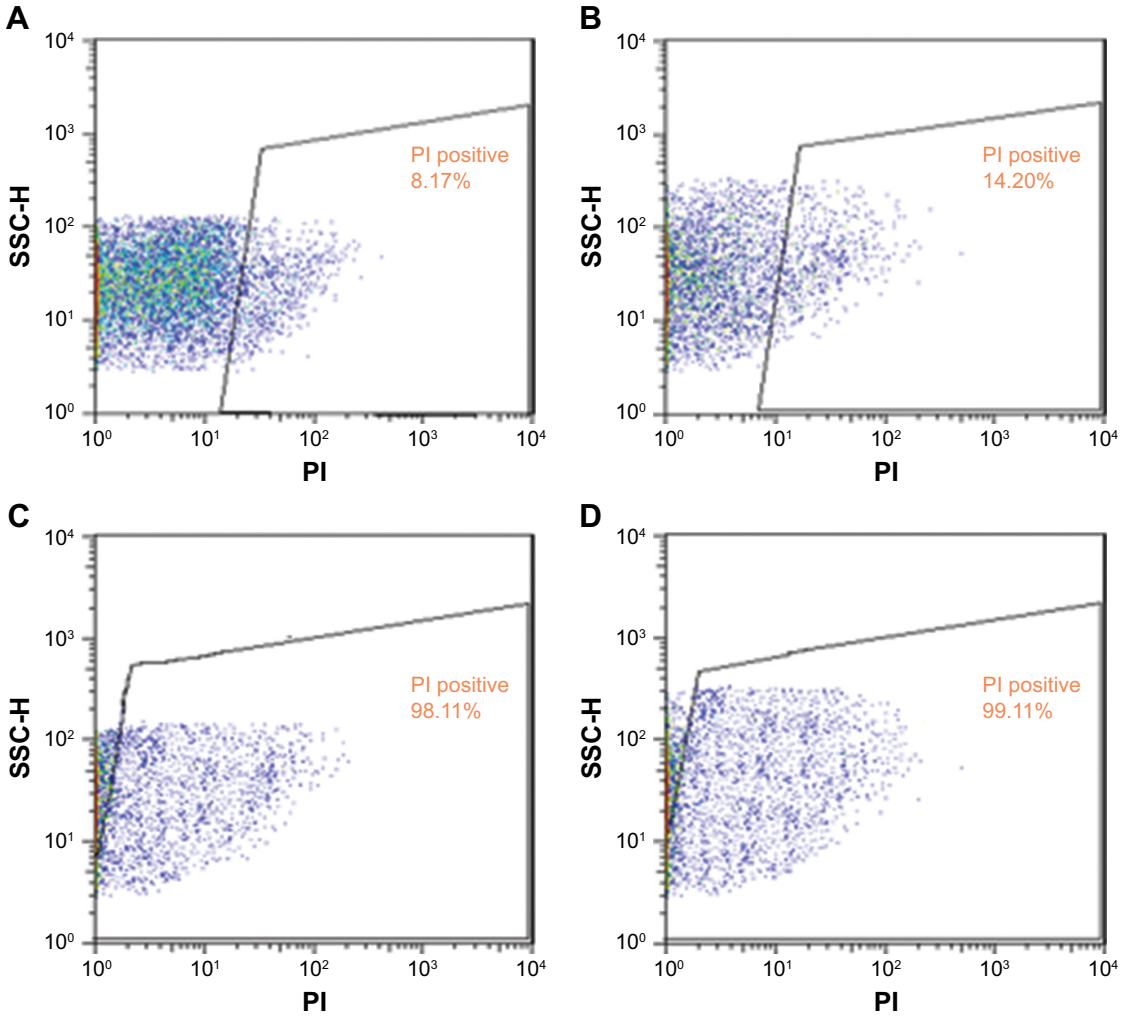

Figure 7 Results flow cytometry analysis (**A**) NSSM-*E. coli*, (**B**) NSSM-*S. aureus*, (**C**) NSSM-MWCNT-*E. coli* and (**D**) NSSM-MWCNT- *S. aureus*.
Abbreviations: PI, propidium iodide; SSC-H, side scatter height.

nanotubes, resulting in disruption of bacterial activity. By increasing the hydrophilicity and the formation layers of water on the sample surface, dead bacteria are desorbed from the surface and do not form a biofilm on the modified membrane. Therefore, these modified membranes become self-cleaning. Membranes based on carbon nanotubes are cleaned regularly, and they can be reused again. So, these modified membranes can be utilized in biomedical and industrial applications with the synergistic effect of absorption and desorption of bacteria off the membrane surface.[26,47,60–62]

Inactivation of *E. coli* bacteria on the modified membranes and reduction of biofilm

The ability of our membrane to absorb and inactivate bacteria was examined. The diameter of *E. coli* was 0.20–1.00 µm, and the mean pore size of the NSSM was 0.20–0.25 µm. A large number of bacteria were passed through the control membrane and formed a colony. The colonies which passed through NSSM in the three experiments were too large and uncountable. Also, some bacteria were absorbed on the unmodified membrane surface and formed biofilm (Figure 6A). In the modified membrane, the size of pores was not larger than the diameter of *E. coli*, so the bacteria could not enter the membrane. Therefore the absorption of bacteria on the modified membrane needed to be studied. FTIR was used to confirm the absorption of bacteria on the modified membrane. Figure 9 shows FTIR of NSSM-MWCNT membrane which was in contact with *E. coli*. The characteristic peaks at 3,100–3,400 cm^{-1} (NH_2, OH stretching), 2,854, and 2,925 (CH stretching), 1,650–1,660 (amid I), 1,520 (amid II), and 1,030–1,150 cm^{-1} (C=O, *P*=O, P–O) confirm that *E. coli* was absorbed on the modified membrane. From Figure 10,

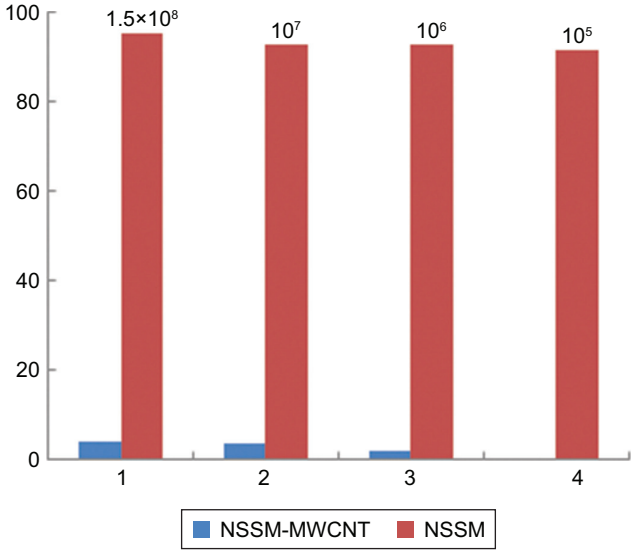

Figure 8 Percentage of bacterial viability in membrane specimens.
Abbreviations: MWCNT, multi-walled carbon nanotube; NSSM, nanoporous solid-state membrane.

a comparison between the modified membrane with carbon nanotube before (A) and after coming into contact with bacteria (B) revealed that a series of pieces and debris are seen on a modified membrane after being in contact with the bacteria. It seems that it is a bacterium that is damaged by carbon nanotube in comparison to normal *E. coli* (C).

The bacteria was absorbed on the modified membrane and came into contact with the carbon nanotubes. As can be seen the bacteria on the modified membrane lost their viability, due to the stylus structure of MWCNT that can penetrate the wall of bacteria. It is also reported that MWCNTs can reduce the metabolic activity of *E. coli*.[63] MWCNT induces serious oxidative stress in bacteria, causing the cell membrane

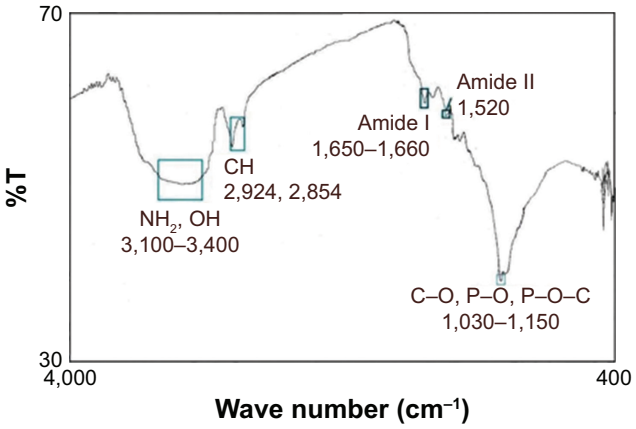

Figure 9 FTIR spectrum of NSSM-MWCNT membrane, which is absorbed by bacteria (1.5×10^8 CFU/mL).
Abbreviations: FTIR, Fourier-transform infrared spectroscopy; MWCNT, multi-walled carbon nanotube; NSSM, nanoporous solid-state membrane.

to become damaged, and the internal cell contents to be released, thus avoiding biofilm formation.[64]

The two parameters of time and concentration for determining the mechanism of bacterial absorption and inactivation are important. Carbon nanotubes' substrates have a porous structure, and there are functional groups and active atoms in their surface. It is expected that bacteria will attach to the modified membranes with a mechanism corresponding to the second order of concentration. To confirm this assumption, the kinetic models were investigated. Absorption of *E. coli* follows the pseudo-second-order kinetic model. Kinetic models are represented by the following equations:[40]

$$\text{Log}\,(q_e - q_t) = \text{Log}\,q_e - \frac{k_1}{2.303}\times t \quad \text{Pseudo-first-order} \tag{7}$$

In the equation q_e and q_t are the absorbed *E. coli* (CFU/g) at time of balance and t (minute), respectively while k_1 is the constant rate (minute^{-1}).

$$\frac{t}{q_t} = \frac{1}{k_2 \times q_e^{\,2}}\ \frac{1}{q_e}\ (t) \quad \text{Pseudo-second-order} \tag{8}$$

In Equation 8 k_2 (CFU^{-1} g minute^{-1}) is the rate constant of absorption. There is a linear relationship between t/q_t and t. The two parameters of k_2 and q_e can be obtained from plotting t/q_t vs t (Figure 11). The correlation of pseudo-first-order (Figure 11A) model is low, and there is a great difference in the absorption capacity of the experimental results and the absorption capacity of calculated results. So, the pseudo-first kinetics model is not suitable to predict the bacteria absorption process. Thus, the phenomenon of absorption of bacteria with the NSSM-MWCNT is not affected by the phenomenon of diffusion.[65] In pseudo-second-order model (Figure 11B), the values of calculated q_e are almost close to the values of experimental q_e. The correlation coefficient is large, which shows the absorption of *E. coli* on NSSM-MWCNT is a second-order reaction and the absorption rate relies on the concentration of the bacteria and the sample surface.[40]

The presence of various functional groups such as OH and COOH on the modified membrane allows the hydrogen bond and other bonds to absorb bacteria. Thus, the Freundlich absorption mechanism is expected to dominate. Isotherm studies were done to investigate the influence of concentration on the process of absorption (Figure 12). The results were compatible with Freundlich model. The Langmuir model

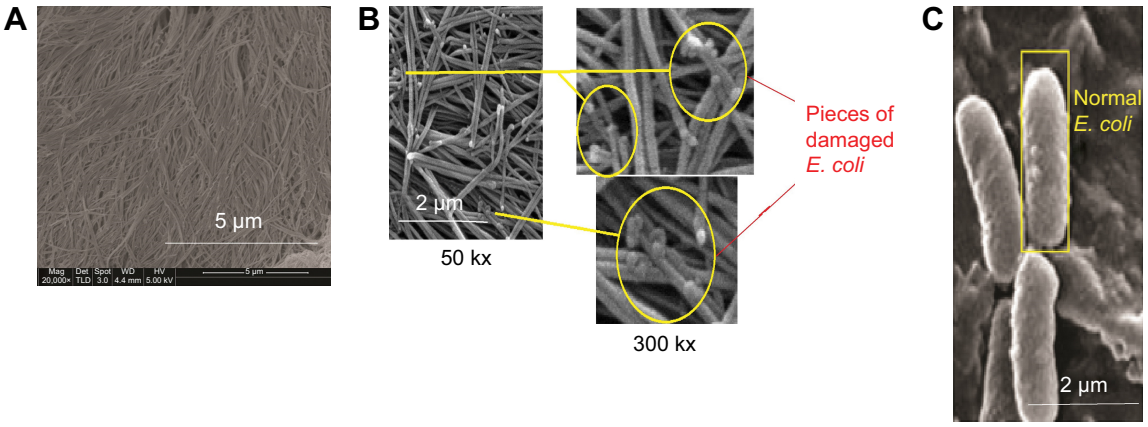

Figure 10 SEM images of membrane modified with carbon nanotube before (**A**) and after coming into contact with bacteria (**B**) and normal *E. coli* (**C**).
Abbreviations: *E. coli*, *Escherichia coli*; SEM, scanning electron microscopy.

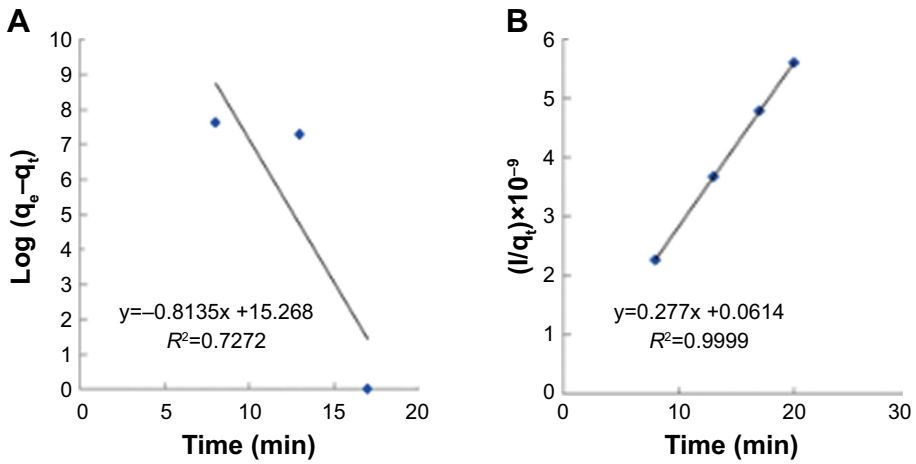

Figure 11 Pesudo-first-order (**A**) and pesudo-second-order (**B**) kinetic models plot for the absorption of *E. coli* of 1.5×10^8 CFU/mL.
Abbreviation: *E. coli*, *Escherichia coli*.

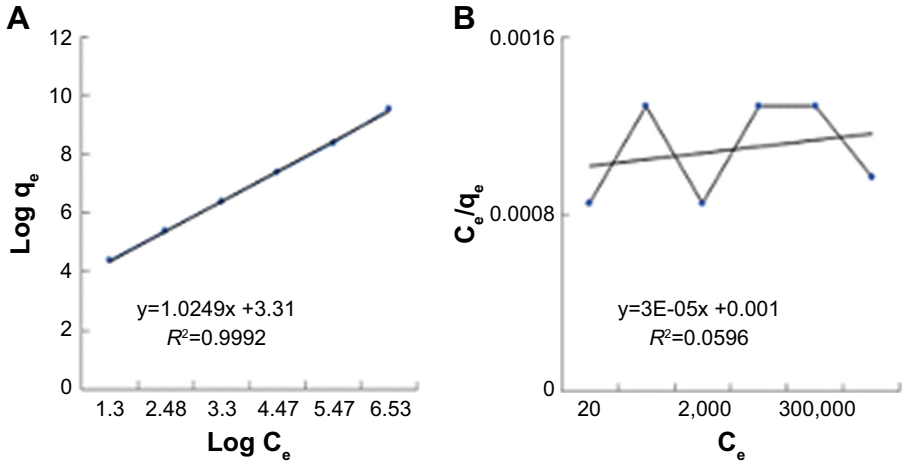

Figure 12 Isotherm models plot (**A**) Freundlich and (**B**) Langmuir for the absorption of *E. coli* at concentrations of 1.5×10^8, 10^7, 10^6, 10^5, 10^4, and 10^3 CFU/mL, 13 minutes and flow rate of 0.05 mL/min.

Table 1 The constants of Freundlich and Langmuir models

Freundlich	Langmuir
R^2=0.99	R^2=0.06
n=0.97	Q_m=3.3×10⁴
K_f=2,047.74	b=0.03

characterized the monolayer absorption on the homogeneous surface which indicates identical sites with the insignificant reaction between adsorbed molecules. Freundlich model is expressed assuming a heterogeneous absorption surface with multilayer absorption. The Langmuir (Equation 7) and Freundlich (Equation 8) equations are represented as follows:

$$\frac{c_e}{q_e} = \frac{1}{BQ_m}\ \frac{c_e}{Q_m} \tag{9}$$

In Equation 9, B is the Langmuir constant (mL/CFU), and Q_m is the theoretical maximum absorption (CFU/g).

$$\text{Log } q_e = \text{Log } k_f \left(\frac{1}{n}\right) \log c_e \tag{10}$$

In Equation 10, q_e is the equilibrium adsorption capacity (CFU/g) and c_e is the balance concentration (CFU/mL).[40] Since n is between 0 and 1, the absorption is multilayered.[65] Based on the Freundlich model, there are several layers of absorption and accumulation of bacteria on the surface of the NSSM-MWCNT. Bacteria are absorbed chemically onto the modified membrane and are inactivated due to the antibacterial properties of carbon nanotubes; therefore they did not form a biofilm. The constants of Freundlich and Langmuir models are presented in Table 1. In chemical absorption, the rate relies on the characterization of adsorbents and absorbed. The size of bacteria is larger than the pores of the MWCNT-NSSM. Therefore the mechanism of diffusion does not interfere with the absorption process.

Table 2 Thermodynamic parameters

Initial concentration 1.5×10⁸ CFU/mL	Temperature °C	% Removal	ΔG kJ/mol
ΔH=171.54 kJ/mol	5	74.00	−2.97
	10	82.00	−6.12
ΔS=0.63 kJ/mol k	15	97.33	−9.27
	20	99.00	−12.42
	30	99.90	−18.72

The results of temperature impact on adsorption of *E. coli* (Table 2) suggested that *E. coli* adsorption was more favorable at higher temperatures.[66] At higher temperatures, *E. coli* tends to form a biofilm layer; thus, the absorption of bacteria on the surface increases.[67] Positive values of entropy (ΔS), and enthalpy changes (ΔH) showed an increase in randomness and endothermic nature of the process respectively, whereas the negative values of free energy confirmed the spontaneous nature and feasibility of the adsorption process.

Conclusion

In this paper, nanoporous membranes were prepared via anodization technique and then modified by carbon nanotubes. The combination of MWCNT with alumina membrane improved the membranes' anti-biofouling properties. The hydrophilic nature of MWCNT enhanced the hydrophilicity of NSSM. Also, the findings of BSA adsorption and the bacterial attachment test showed that the MWCNT-NSSM with nano-roughness had superior biofouling resistance. Also, the result showed that bacteria were absorbed onto the modified membrane with second-order kinetics without diffusion, following Freundlich adsorption isotherm model.

The following supplementary data are also available in the Supplementary materials:

- a schematic diagram of the membranes' fabrication;
- the parameters of Van Oss method;
- a schematic diagram of plate count method.

Acknowledgment

Our research group appreciates all those who collaborated with us on this project.

Disclosure

The authors report no conflicts of interest in this work.

References

1. Lee W, Ji R, Gösele U, Nielsch K. Fast fabrication of long-range ordered porous alumina membranes by hard anodization. *Nat Mater*. 2006;5(9):741–747.
2. Colombo P. In praise of pores. *Science*. 2008:381–383.
3. Davis ME. Ordered porous materials for emerging applications. *Nature*. 2002;417(6891):813–821.
4. Vlassiouk I, Krasnoslobodtsev A, Smirnov S, Germann M. "Direct" Detection and Separation of DNA Using Nanoporous Alumina Filters. *Langmuir*. 2004;20(23):9913–9915.
5. Vlassiouk I, Takmakov P, Smirnov S. Sensing DNA hybridization via ionic conductance through a nanoporous electrode. *Langmuir*. 2005; 21(11):4776–4778.
6. Popat KC, Mor G, Grimes CA, Desai TA. Surface modification of nanoporous alumina surfaces with Poly(ethylene glycol). *Langmuir*. 2004; 20(19):8035–8041.

7. Wu S, Ye W, Yang M, et al. Impedance sensing of DNA immobilization and hybridization by microfabricated alumina nanopore membranes. *Sensors Actuators B Chem*. 2015;216:105–112.
8. Tian F, Lyu J, Shi J, Tan F, Yang M. A polymeric microfluidic device integrated with nanoporous alumina membranes for simultaneous detection of multiple foodborne pathogens. *Sens Actuators B Chem*. 2016;225:312–318.
9. Choi S, Chae J. Methods of reducing non-specific adsorption in microfluidic biosensors. *J Micromech Microeng*. 2010;20(7):075015.
10. Percival SL, Suleman L, Vuotto C, Donelli G. Healthcare-associated infections, medical devices and biofilms: risk, tolerance and control. *J Med Microbiol*. 2015;64(Pt 4):323–334.
11. Hilal N, Al-Khatib L, Atkin BP, Kochkodan V, Potapchenko N. Photochemical modification of membrane surfaces for (bio)fouling reduction: a nano-scale study using AFM. *Desalination*. 2003;158(1–3):65–72.
12. Narayan RJ, Adiga SP, Pellin MJ, et al. Atomic layer deposition-based functionalization of materials for medical and environmental health applications. *Phil Trans Math, Phys Eng Sci*. 2010;368(1917): 2033–2064.
13. Lee SB, Mitchell DT, Trofin L, Nevanen TK, Soderlund H, Martin CR. Antibody-based bio-nanotube membranes for enantiomeric drug separations. *Science*. 2002;296(5576):2198–2200.
14. Velleman L, Triani G, Evans PJ, Shapter JG, Losic D. Structural and chemical modification of porous alumina membranes. *Microporous Mesoporous Mater*. 2009;126(1–2):87–94.
15. Losic D, Cole MA, Dollmann B, Vasilev K, Griesser HJ. Surface modification of nanoporous alumina membranes by plasma polymerization. *Nanotechnology*. 2008;19(24):245704.
16. Garrett DJ, Ganesan K, Stacey A, Fox K, Meffin H, Prawer S. Ultrananocrystalline diamond electrodes: optimization towards neural stimulation applications. *J Neural Eng*. 2012;9(1):016002.
17. Ahn CH, Baek Y, Lee C, et al. Carbon nanotube-based membranes: fabrication and application to desalination. *J Ind Eng Chem*. 2012;18(5): 1551–1559.
18. Gilani N, Daryan JT, Rashidi A, Omidkhah MR. Separation of methane–nitrogen mixtures using synthesis vertically aligned carbon nanotube membranes. *Appl Surf Sci*. 2012;258(10):4819–4825.
19. Hou P, Liu C, Shi C, Cheng H. Carbon nanotubes prepared by anodic aluminum oxide template method. *Chin Sci Bull*. 2012;57(2–3):187–204.
20. Srivastava A, Srivastava ON, Talapatra S, Vajtai R, Ajayan PM. Carbon nanotube filters. *Nat Mater*. 2004;3(9):610–614.
21. Kang S, Pinault M, Pfefferle LD, Elimelech M. Single-walled carbon nanotubes exhibit strong antimicrobial activity. *Langmuir*. 2007; 23(17):8670–8673.
22. Kang S, Herzberg M, Rodrigues DF, Elimelech M. Antibacterial effects of carbon nanotubes: size does matter! *Langmuir*. 2008;24(13): 6409–6413.
23. Das R, Ali ME, Hamid SBA, Ramakrishna S, Chowdhury ZZ. Carbon nanotube membranes for water purification: a bright future in water desalination. *Desalination*. 2014;336:97–109.
24. Shuval H. Estimating the global burden of thalassogenic diseases: human infectious diseases caused by wastewater pollution of the marine environment. *J Water Health*. 2003;1(2):53–64.
25. Orooji Y, Faghih M, Razmjou A, et al. Nanostructured mesoporous carbon polyethersulfone composite ultrafiltration membrane with significantly low protein adsorption and bacterial adhesion. *Carbon*. 2017;111:689–704.
26. Upadhyayula VK, Deng S, Mitchell MC, Smith GB, Nair VK, Ghoshroy S. Adsorption kinetics of *Escherichia coli* and Staphylococcus aureus on single-walled carbon nanotube aggregates. *Water Sci Technol*. 2008;58(1):179–184.
27. Van Oss CJ, Chaudhury MK, Good RJ. Monopolar surfaces. *Adv Colloid Interface Sci*. 1987;28(1):35–64.
28. Van Oss CJ, Ju L, Chaudhury MK, Good RJ. Estimation of the polar parameters of the surface tension of liquids by contact angle measurements on gels. *J Colloid Interface Sci*. 1989;128(2):313–319.
29. Zhao S, Wang Z, Wei X, et al. Performance improvement of polysulfone ultrafiltration membrane using PANiEB as both pore forming agent and hydrophilic modifier. *J Memb Sci*. 2011;385–386:251–262.
30. Razmjou A, Mansouri J, Chen V, Lim M, Amal R. Titania nanocomposite polyethersulfone ultrafiltration membranes fabricated using a low temperature hydrothermal coating process. *J Memb Sci*. 2011; 380(1–2):98–113.
31. Razmjou A, Mansouri J, Chen V. The effects of mechanical and chemical modification of TiO2 nanoparticles on the surface chemistry, structure and fouling performance of PEs ultrafiltration membranes. *J Memb Sci*. 2011;378(1–2):73–84.
32. Davey ME, O'Toole GA. Microbial biofilms: from ecology to molecular genetics. *Microbiol Mol Biol Rev*. 2000;64(4):847–867.
33. Kaper JB, Nataro JP, Mobley HLT. Pathogenic *Escherichia coli*. *Nat Rev Microbiol*. 2004;2(2):123–140.
34. O'Gara JP. ica and beyond: biofilm mechanisms and regulation in *Staphylococcus epidermidis* and *Staphylococcus aureus*. *FEMS Microbiol Lett*. 2007;270(2):179–188.
35. Moazzam P, Razmjou A, Golabi M, Shokri D, Landarani-Isfahani A. Investigating the BSA protein adsorption and bacterial adhesion of Al-alloy surfaces after creating a hierarchical (micro/nano) superhydrophobic structure. *J Biomed Mater Res*. 2016;104(9):2220–2233.
36. Orooji Y, Liang F, Razmjou A, et al. Excellent Biofouling Alleviation of Thermoexfoliated Vermiculite Blended Poly(ether sulfone) Ultrafiltration Membrane. *ACS Appl Mater Interfaces*. 2017;9(35):30024–30034.
37. Orooji Y, Liang F, Razmjou A, Liu G, Jin W. Preparation of anti-adhesion and bacterial destructive polymeric ultrafiltration membranes using modified mesoporous carbon. *Separ Purif Tech*. 2018;205:273–283.
38. Pezeshkpour V, Khosravani SA, Ghaedi M, et al. Ultrasound assisted extraction of phenolic acids from broccoli vegetable and using sonochemistry for preparation of MOF-5 nanocubes: comparative study based on micro-dilution broth and plate count method for synergism antibacterial effect. *Ultrason Sonochem*. 2018;40:1031–1038.
39. Shokrollahi A, Ghaedi M, Ranjbar M, Alizadeh A. Kinetic and thermodynamic studies of the removal of murexide from aqueous solutions on to activated carbon. *J Iran Chem Res*. 3:219.
40. Shokrollahi A, Alizadeh A, Malekhosseini Z, Ranjbar M. Removal of bromocresol green from aqueous solution via adsorption on *Ziziphus nummularia* as a new, natural, and low-cost adsorbent: kinetic and thermodynamic study of removal process. *J Chem Eng Data*. 2011;56(10): 3738–3746.
41. Penumetcha S, Kona R, Hardin J, Molder A, Steinle E. Monitoring transport across modified nanoporous alumina membranes. *Sensors*. 2007;7(11):2942–2952.
42. Leitao DC, Ventura J, Sousa CT, et al. Tailoring the physical properties of thin nanohole arrays grown on flat anodic aluminum oxide templates. *Nanotechnology*. 2012;23(42):425701.
43. Norek M, Krasiński A. Controlling of water wettability by structural and chemical modification of porous anodic alumina (Paa): towards super-hydrophobic surfaces. *Surf Coating Tech*. 2015;276:464–470.
44. Boussu K, van der Bruggen B, Volodin A, et al. Characterization of commercial nanofiltration membranes and comparison with self-made polyethersulfone membranes. *Desalination*. 2006;191(1–3): 245–253.
45. Zhu YY, Ding GQ, Ding JN, Yuan NY. AFM, SEM and TEM studies on porous anodic alumina. *Nanoscale Res Lett*. 2010;5(4):725–734.
46. Zheng J, Li L, Chen S, Jiang S. Molecular simulation study of water interactions with oligo (ethylene glycol)-terminated alkanethiol self-assembled monolayers. *Langmuir*. 2004;20(20):8931–8938.
47. Elbahri M, Paretkar D, Hirmas K, Jebril S, Adelung R. Anti-Lotus effect for Nanostructuring at the Leidenfrost temperature. *Adv Mater*. 2007;19(9):1262–1266.
48. Kubiak KJ, Wilson MCT, Mathia TG, Carval P. Wettability versus roughness of engineering surfaces. *Wear*. 2011;271(3–4):523–528.
49. Scopelliti PE, Borgonovo A, Indrieri M, et al. The effect of surface nanometre-scale morphology on protein adsorption. *PLoS One*. 5(7):e11862.

50. Pertsin AJ, Grunze M. Computer simulation of water near the Surface of Oligo(ethylene glycol)-terminated alkanethiol self-assembled monolayers. *Langmuir*. 2000;16(23):8829–8841.
51. Archambault JG, Brash JL. Protein repellent polyurethane-urea surfaces by chemical grafting of hydroxyl-terminated poly(ethylene oxide): effects of protein size and charge. *Colloids Surf B Biointerfaces*. 2004;33(2):111–120.
52. Hou J, Dong G, Ye Y, Chen V. Enzymatic degradation of Bisphenol-A with immobilized laccase on TiO2 sol–gel coated PVDF membrane. *J Membr Sci*. 2014;469:19–30.
53. Cho K-H, Park J-E, Osaka T, Park S-G. The study of antimicrobial activity and preservative effects of nanosilver ingredient. *Electrochimica Acta*. 2005;51(5):956–960.
54. Harris LG, Foster SJ, Richards RG. An introduction to Staphylococcus aureus, and techniques for identifying and quantifying S. aureus adhesins in relation to adhesion to biomaterials: review. *Eur Cell Mater*. 2002;4(3):39–60.
55. Ke X, Huang Y, Dargaville TR, Fan Y, Cui Z, Zhu H. Modified alumina nanofiber membranes for protein separation. *Separ Purif Tech*. 2013; 120:239–244.
56. Chayen NE, Saridakis E, Sear RP. Experiment and theory for heterogeneous nucleation of protein crystals in a porous medium. *Proc Natl Acad Sci USA*. 2006;103(3):597–601.
57. Rokni N. Principal of nutrition material health. *Pub Ins University of Tehran*. 1999;3:10–11.
58. Barot MS, Mosenthal AC, Bokkenheuser VD. Location of Campylobacter jejuni in infected chicken livers. *J Clin Microbiol*. 1983;17(5): 921–922.
59. Kheyri A, Fakhernia M, Haghighat-Afshar N, et al. Microbial contamination of meat products produced in the factories of West Azerbaijan Province, North West of Iran. *Global Veterinaria*. 2014;12(6):796–802.
60. Huh AJ, Kwon YJ. "Nanoantibiotics": A new paradigm for treating infectious diseases using nanomaterials in the antibiotics resistant era. *J Contr Release*. 2011;156(2):128–145.
61. Upadhyayula VKK, Deng S, Mitchell MC, Smith GB. Application of carbon nanotube technology for removal of contaminants in drinking water: a review. *Sci Total Environ*. 2009;408(1):1–13.
62. Rai M, Yadav A, Gade A. Silver nanoparticles as a new generation of antimicrobials. *Biotechnol Adv*. 2009;27(1):76–83.
63. Allen C, Loo JF, Yu S, Kong S, Chan T-F. Monitoring bacterial growth using tunable resistive pulse sensing with a pore-based technique. *Appl Microbiol Biotechnol*. 2014;98(2):855–862.
64. Brady-Estévez AS, Kang S, Elimelech M. A single-walled-carbon-nanotube filter for removal of viral and bacterial pathogens. *Small*. 2008;4(4):481–484.
65. Patel R, Suresh S. Kinetic and equilibrium studies on the biosorption of reactive black 5 dye by *Aspergillus foetidus*. *Bioresour Technol*. 2008;99(1):51–58.
66. Hooshyari G. Evaluating filter materials for E. coli removal from Stormwater. 2017. Electronic Theses and Dissertations. 1206. Available from: https://openprairie.sdstate.edu/etd/.
67. Patil SA, Harnisch F, Kapadnis B, Schröder U. Electroactive mixed culture biofilms in microbial bioelectrochemical systems: the role of temperature for biofilm formation and performance. *Biosens Bioelectron*. 2010;26(2):803–808.

Supplementary materials

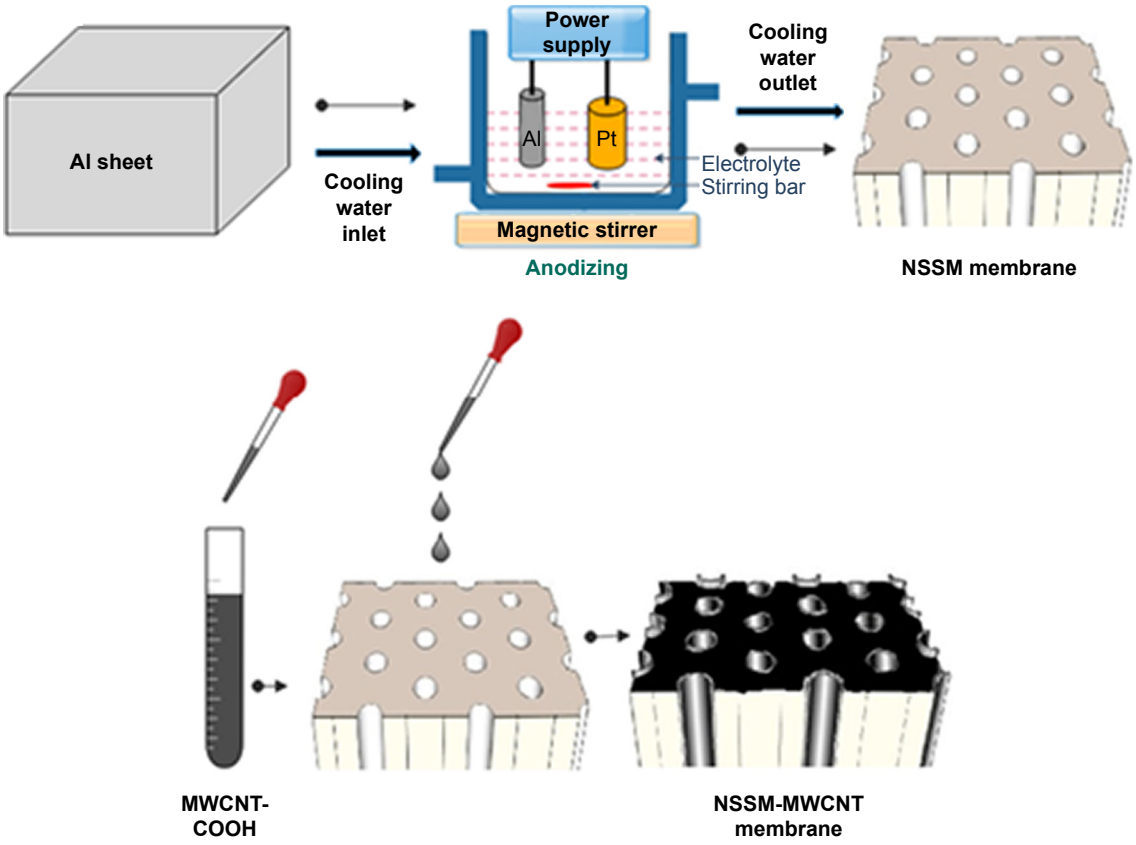

Figure S1 The general schematic diagram of the fabrication and modification process of membranes.
Abbreviations: MWCNT, multi-walled carbon nanotube; NSSM, nanoporous solid-state membrane.

Table S1 Parameters of acid-base Van Oss method

Liquid	SFT (mN/m)	$\sigma^{disperse}$ (mN/m)	Acid (mN/m)	Base (mN/m)
Milli-Q water	72.8	21.8	25.5	25.5
Glycerol	64.0	34.0	3.9	57.4
Formamide	58.0	39.0	23.2	23.2

Abbreviation: SFT, surface free energy.

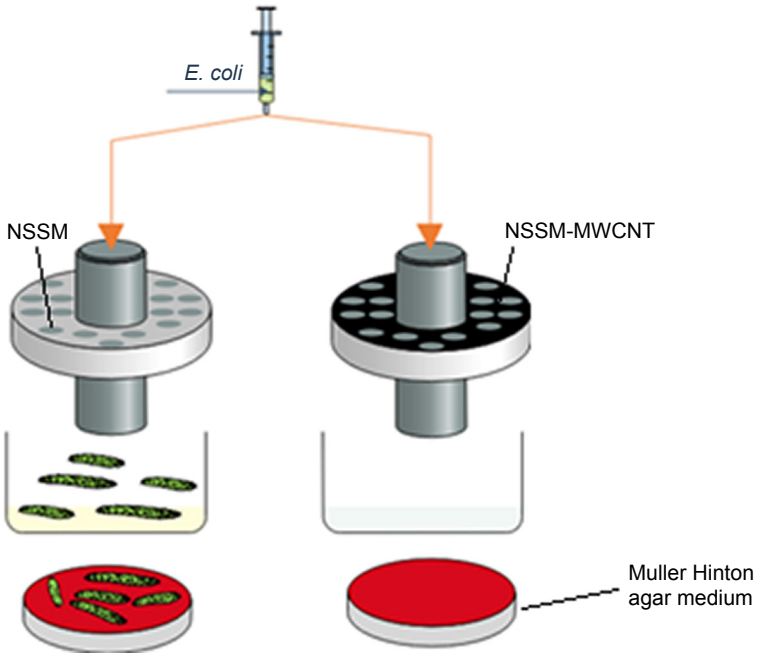

Figure S2 Absorption of *E. coli* on the membranes in dead-end cell.
Abbreviations: *E. coli*, *Escherichia coli*; MWCNT, multi-walled carbon nanotube; NSSM, nanoporous solid-state membrane.

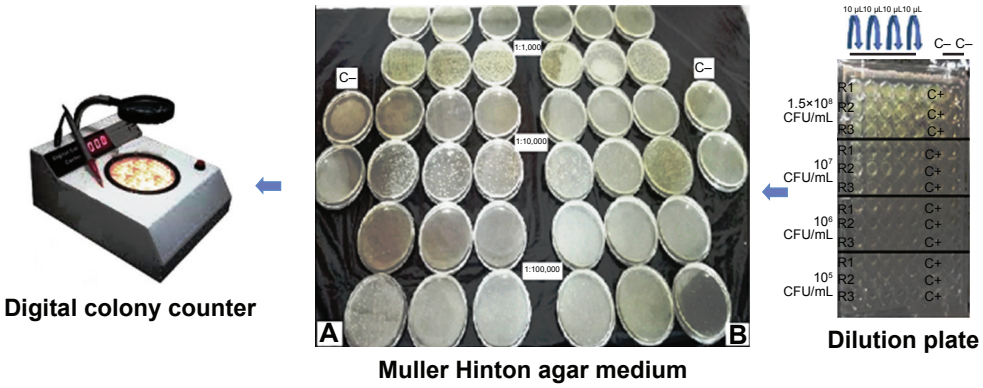

Figure S3 Plate count method in absorption studies.
Note: Counting the colonies of concentration (**A**) 1.5×10^8 and (**B**) 10^7.